

FTIR Identification of the $\nu_4(\sigma_u)$ and $\nu_6(\pi_u)$ Modes of Linear GeC_3Ge Trapped in Solid Ar

Eric Gonzalez, C. M. L. Rittby, and W. R. M. Graham*

Department of Physics and Astronomy, Texas Christian University, Fort Worth, Texas 76129

Received: July 18, 2008; Revised Manuscript Received: September 05, 2008

GeC_3Ge was previously¹ produced by the dual laser ablation of germanium and carbon rods, and the $\nu_3(\sigma_u)$ carbon–carbon stretching fundamental was assigned at 1920.7 cm^{-1} . This paper presents results from new experiments that have enhanced the production of the molecule via laser ablation of a single sintered germanium–carbon rod, thus enabling the identification of two additional infrared active vibrational fundamentals. Ge participates strongly in one of these, the $\nu_4(\sigma_u)$ mode, and the corresponding Ge isotopic shifts reported here are the first for a germanium–carbon species. GeC_3Ge was produced by trapping the products from the laser evaporation of the Ge–C rod, in solid Ar at $\sim 10\text{ K}$, and recording the FTIR (Fourier transform infrared) spectra. Comparison of ^{70,72,73,74,76}Ge and ¹³C isotopic shift measurements with the predictions of density functional theory calculations (DFT) at the B3LYP/cc-pVDZ level confirms the identification of the $\nu_4(\sigma_u)$ stretching fundamental at 735.3 cm^{-1} and the $\nu_6(\pi_u)$ bending fundamental at 580.1 cm^{-1} for linear GeC_3Ge .

1. Introduction

Carbon, silicon, and germanium are the components of many optoelectronic, semiconductor, and nano materials.^{2–5} It is therefore of interest to form and characterize the spectra of new C/Ge/Si molecules which could be the building blocks for novel structures with potential future applications in these technologies. Previously, our group has reported vibrational spectra for Si_nC_m ,^{6,7} Ge_nC_m ,^{1,8} and $\text{Si}_n\text{C}_m\text{Ge}_l$ ⁹ clusters. In early work, novel small silicon–carbon clusters were produced by the evaporation of mixtures of silicon and carbon from tantalum Knudsen cells. Vibrational fundamentals were identified for a variety of Si_nC_m clusters with various structures, including linear SiC_3Si ,¹⁰ cyclic Si_2C_2 ,¹¹ and planar pentagonal Si_3C_2 .¹² Later investigations, using the laser ablation technique, identified for the first time vibrational fundamentals of the larger silicon–carbon clusters SiC_7 and SiC_9 ,^{6,7} as well as the germanium–carbon species GeC_3Ge ,¹ GeC_7 , and GeC_9 ,⁸ and the mixed Group IV cluster, GeC_3Si .⁹

FTIR matrix isolation studies on the vibrational spectra of Ge_nC_m clusters formed by laser ablation have continued. Efforts have been directed toward increasing the production of GeC_3Ge to be able to detect the next most intense infrared active modes, which were not detectable when the $\nu_3(\sigma_u) = 1920.7\text{ cm}^{-1}$ fundamental was produced for the first time.¹ This was achieved by sintering a germanium–carbon rod, which upon laser ablation produced a very high yield of the molecule. By using hard, sintered Ge–C rods evaporation was enhanced over sputtering, allowing long deposition times which resulted in trapping more molecules in the matrix.

In comparing measured isotopic shifts to the pattern predicted by DFT calculations, our group usually scales the theoretical shifts by multiplying by the ratio of the experimental and calculated main band frequencies. In general, the criterion for good agreement is that the differences between the experimental and scaled theoretical frequency shifts are less than 2 cm^{-1} . Since the Ge isotopic shift envelope extends to only a few cm^{-1} ,

TABLE 1: DFT-B3LYP/cc-pVDZ Predicted Vibrational Frequencies (cm^{-1}) and Band Intensities for Linear GeC_3Ge

vib mode	freq (cm^{-1})	IR intensity (km/mol)
$\nu_1(\sigma_g)$	1520.4	0
$\nu_2(\sigma_g)$	277.2	0
$\nu_3(\sigma_u)$	2028.1	2226
$\nu_4(\sigma_u)$	740.0	217
$\nu_5(\pi_g)$	190.4	0
$\nu_6(\pi_u)$	575.4	16
$\nu_7(\pi_u)$	69.1	4

this criterion could not be used in the present work. Instead, a new way to correlate the theoretical frequency shifts was used to compare experiment and theory, which is presented in the Theory section.

This paper presents experimental measurements and DFT calculations, which corroborate the linear geometry already determined for GeC_3Ge in its ground state. On the basis of very good agreement between ^{70,72,73,74,76}Ge and ¹³C isotopic shift measurements and the predictions of DFT calculations the $\nu_4(\sigma_u)$ and $\nu_6(\pi_u)$ fundamentals of GeC_3Ge have now been unambiguously assigned at 735.3 and 580.1 cm^{-1} , respectively.

2. Theory

The B3LYP^{13–15} functional (Becke type 3 exchange and the correlation functional of Lee, Yang, and Parr) with cc-pVDZ basis was used in calculations with the GAUSSIAN 03 program suite.¹⁶ Table 1 lists the predicted harmonic fundamental frequencies and infrared intensities. The infrared active vibrations, showing normal mode displacements, are presented in Figure 1. In our earlier work on GeC_3Ge (ref 1) the 6-31G* basis was used, while in later studies on GeC_7 and GeC_9 ⁸ and GeC_3Si ⁹ the basis set used was cc-pVDZ. It should be noted that with the 6-31G* basis set the bending fundamentals are generally predicted at considerably higher frequencies than when using the cc-pVDZ basis. Accordingly, the $\nu_6(\pi_u)$ fundamental of GeC_3Ge , which is predicted at 933 cm^{-1} with the 6-31G* basis set (see ref 1) is calculated at 575.4 cm^{-1} with the cc-

* To whom correspondence should be addressed: TCU Box 298840, Fort Worth, TX 76129. E-mail: w.graham@tcu.edu..

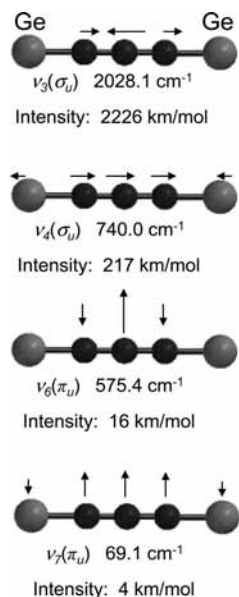


Figure 1. DFT-B3LYP/cc-pVDZ predicted infrared active vibrational frequencies (cm^{-1}) and band intensities for $^1\Sigma_g^+$ ground state of linear GeC_3Ge . Arrows indicate the principal nuclear displacements for each mode.

pVDZ basis set. In extensive studies of many carbon,^{17–19} silicon–carbon,^{6,7} and germanium–carbon⁸ species it has been found that calculations with the cc-pVDZ basis set provide a good description of geometries and vibrational fundamentals. Experimental measurement of the $\nu_6(\pi_u)$ mode of GeC_3Ge in the present work confirms the superiority of the cc-pVDZ basis over the 6-31G* basis set (see Results and Analysis). Theoretical studies²⁰ on Ge_2C_3 by using DFT, MP2, and CCSD(T) with larger basis sets predicts the linear GeC_3Ge as the lowest energy isomer.

3. Calculation of Isotopic Shifts

The standard approach when calculating isotopic shifts for carbon clusters is to obtain them from the diagonalization of the appropriately mass-weighted force constant matrix. When anharmonic effects as well as effects due to couplings with other vibrational modes are small such shifts typically agree with experiment to within a few tenths of cm^{-1} . Larger errors can be attributed to inaccuracies in the force constant matrix giving rise to errors in the normal mode coordinates for the vibrational fundamental being observed. Below we have calculated the isotopic shifts resulting from ^{13}C substitution using this standard approach.

The proposed identification of the $\nu_4(\sigma_u)$ fundamental of GeC_3Ge , however, allows us to consider the shifts due to the various isotopes of germanium using a different approach. The perturbation resulting from changes in the molecule's nuclear masses caused by isotopic substitution is the difference between the kinetic energy of the final mass, $m_n(f)$ and the initial mass, $m_n(i)$, for all K isotopically substituted atoms,

$$W(i \rightarrow f) = \sum_{n=1}^K \left[\frac{\hbar^2}{2m_n(i)} \nabla_n^2 - \frac{\hbar^2}{2m_n(f)} \nabla_n^2 \right] \quad (1)$$

By using this perturbation and neglecting coupling between other vibrational modes, the harmonic frequency ω , shifted from the unperturbed frequency ω_0 , resulting from an isotopic substitution, can be derived to infinite order to be given by

$$\omega = \left[1 - \sum_{n=1}^K \left(1 - \frac{m_n(i)}{m_n(f)} \right) |\mathbf{u}_n|^2 \right]^{1/2} \omega_0 \quad (2)$$

where \mathbf{u}_n is the normal mode displacement vector of atom n in normalized mass weighted coordinates. Within the harmonic approximation therefore, the inexactness in eq 2 originates only with the values of the normal mode displacements providing the interaction with other fundamentals can be neglected. In the case of the germanium shifts of the $\nu_4(\sigma_u)$ fundamental of GeC_3Ge , eq 2 was found to be applicable since the isotopic shifts calculated with eq 2 agreed to within 0.01 cm^{-1} with the shifts calculated with the standard method employing the full force constant matrix. In addition, since the two germanium atoms are equivalent, eq 2 now provides a simple one-parameter model by which we can fit calculated isotopic shifts to experimental shifts, thus giving us an improved value of the mass-weighted normal mode displacement.

4. Experimental Procedure

The objective of this research was to increase the yield of linear GeC_3Ge in order to improve the signal-to-noise ratio and enable the measurement of $\nu_4(\sigma_u)$ and $\nu_6(\pi_u)$ that are predicted to be the next most intense vibrational fundamentals after the $\nu_3(\sigma_u)$ fundamental already reported. In our previous study,¹ GeC_3Ge was first produced by simultaneously ablating the surfaces of a pair of continuously rotating and translating germanium and carbon rods; however, in the present work, this dual laser ablation approach was replaced by evaporating a single rod made from a mixture of Ge and C. The ablation of a rod containing a mixture of Ge, Si, and C was first used to produce GeC_3Si .⁹ In the present work, optimizing the Ge:C mass ratio of the germanium–carbon rod was crucial to achieving a high yield of GeC_3Ge . From a series of experiments testing different ratios to enhance the production of this molecule, it was concluded that the mass ratio Ge:C = 1.5:1 was optimum.

Products were evaporated from a sintered germanium–carbon rod with the use of a Nd:YAG laser (Spectra Physics) operating at 1064 nm in pulse mode. The evaporated species were condensed in solid Ar (Matheson, 99.9995% purity) on a gold surfaced mirror previously cooled to $\sim 10 \text{ K}$ by a closed refrigeration system (ARS, Displex). The mirror was enclosed in a vacuum chamber maintained at a pressure of $\sim 10^{-8}$ Torr. Experimental parameters such as the laser focus, laser power, and Ar flow were adjusted to favor the production of GeC_3Ge . For the laser ablation of the rod a beam with a power of 3.0 W, loosely focused on an area of $\sim 25 \text{ mm}^2$, was used. During deposition, the Ar flow rate used was $\sim 1 \text{ mmol/h}$. Typically, matrix samples were deposited for 2 h.

To make an unambiguous determination of molecular structure and to identify vibrational fundamentals it is crucial to measure isotopic shifts. For this reason Ge–C rods were fabricated with mixtures of ^{12}C (Alfa Aesar, 99.9995% purity) and ^{13}C (Isotec, 99.3% purity). Since, as mentioned earlier, Ge has five naturally occurring isotopes, Ge isotopic enrichment was not necessary. Two rods were fabricated with the mass ratio Ge:C = 1.5:1, one with ^{12}C and the other having an appropriate ^{13}C enrichment to obtain the ^{13}C isotopic shifts necessary to determine the number of carbon atoms present and the geometry of the molecule.

FTIR absorption spectra of the products condensed in the Ar matrix were recorded over the range of $500\text{--}3500 \text{ cm}^{-1}$ at a resolution of 0.2 cm^{-1} , using a Bomem DA3.16 Fourier transform spectrometer equipped with a liquid nitrogen cooled

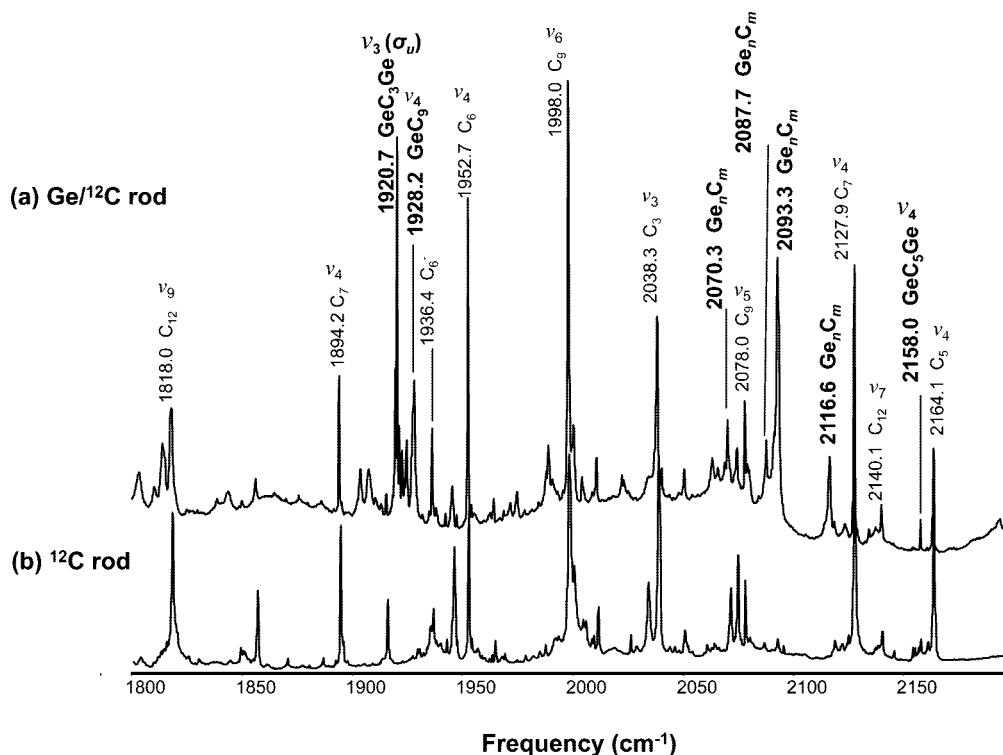


Figure 2. FTIR spectra produced by the ablation of (a) a germanium–carbon rod and (b) a pure ¹²C rod in the 1800–2150 cm⁻¹ frequency region.

Hg–Cd–Te (MCT) detector and KBr beamsplitter. Details of the optical system have been reported previously.²¹

5. Results and Discussion

Figure 2 shows survey spectra recorded in the range 1800–2200 cm⁻¹ where the most intense stretching modes of germanium–carbon clusters are expected to be located. The spectrum produced by the ablation of a germanium–carbon rod is shown in Figure 2a. For comparison, Figure 2b shows the spectrum produced under identical experimental conditions by the ablation of a carbon rod alone. The germanium–carbon rod ablation produced the characteristic fundamental vibrations of germanium–carbon clusters identified in our previous studies, the $\nu_4(\sigma)$ mode of GeC₉ at 1928.2 cm⁻¹,⁸ the $\nu_4(\sigma_u)$ mode of GeC₅Ge at 2158.0 cm⁻¹,²² and the $\nu_3(\sigma_u)$ mode of GeC₃Ge at 1920.7 cm⁻¹.¹ In addition, other new absorptions at 2087.7, 2093.3, and 2116.6 cm⁻¹ were observed, which are currently under investigation and will be the subjects of future reports. Figure 3 shows the spectra in the range of 500–800 cm⁻¹ where three other new bands appear, a sharp pair of lines at 579.1 and 580.1 cm⁻¹ and a broader band at 736.0 cm⁻¹ which we will consider first.

GeC₃Ge is a prominent species in the spectrum in Figure 2 judging by the band strength of the most intense mode of GeC₃Ge at $\nu_3(\sigma_u) = 1920.7$ cm⁻¹ compared with the absorptions of other species. The 736.0 cm⁻¹ absorption is close to the 740.0 cm⁻¹ frequency predicted for the $\nu_4(\sigma_u)$ fundamental, and the ratio of its intensity to the $\nu_3(\sigma_u)$ band is 0.3, reasonably close to the ratio of 0.1 calculated from the predicted intensities of the fundamentals shown in Table 1. It thus appears possible that this band corresponds to the $\nu_4(\sigma_u)$ stretching fundamental of linear GeC₃Ge.

Since Ge participates in the next most intense $\nu_4(\sigma_u)$ vibrational mode (see Figure 1), and has five natural isotopes with relative abundances of 21.2% ⁷⁰Ge, 27.7% ⁷²Ge, 7.7% ⁷³Ge,

35.9% ⁷⁴Ge, and 7.4% ⁷⁶Ge, there are 15 possibly observable isotopomers of GeC₃Ge even in the absence of ¹³C isotopic substitutions. The natural abundances of the Ge isotopes produce a Ge isotopic shift pattern on the envelope of the $\nu_4(\sigma_u)$ absorption that is consistent with the presence of two equivalent Ge atoms. The absorption envelope of the $\nu_4(\sigma_u)$ fundamental of linear GeC₃Ge would be expected to contain several peaks and extend over ~ 5 cm⁻¹. The envelope's characteristic shape would result from the Ge atoms' participation in the vibration, the frequency, the normal mode displacement vector **u** (see eq 2), and the line widths of the germanium isotopomer peaks contributing to the absorption envelope. Fifteen isotopomers mentioned above have different probabilities of being formed. For example, the 74-12-12-12-72, 74-12-12-12-70, and 74-12-12-12-74 isotopomers have probabilities 0.20, 0.15, and 0.13, respectively, while the 76-12-12-12-76 and 76-12-12-12-73 isotopomers have relatively lower probabilities, 0.006 and 0.01, respectively. Consequently, the peaks of some isotopomers would be more intense than others because of their greater abundances. The vibrational frequency value and normal mode displacement vector **u** determine the spread of the absorption envelope. In the 700 cm⁻¹ region it is spread over only ~ 5 cm⁻¹, compared with tens of cm⁻¹ if the absorption were in the 2000 cm⁻¹ region. The peak line widths determine the number of peaks resolved. If line widths are close to the spectrometer resolution (0.2 cm⁻¹) all peaks would be resolved, but if line widths are greater than the resolution and the envelope extends only a few cm⁻¹, many peaks would be unresolved.

With the assumption that the spectrum originates from the $\nu_4(\sigma_u)$ fundamental of linear GeC₃Ge we chose the unperturbed frequency in eq 2 to correspond to the 74-12-12-12-74 isotopomer observed at 735.3 cm⁻¹ (see Table 2). Using the normal mode displacement from our DFT calculation proved to result in an absorption envelope that was substantially broader than the one observed in the experimental spectrum. To ascertain if

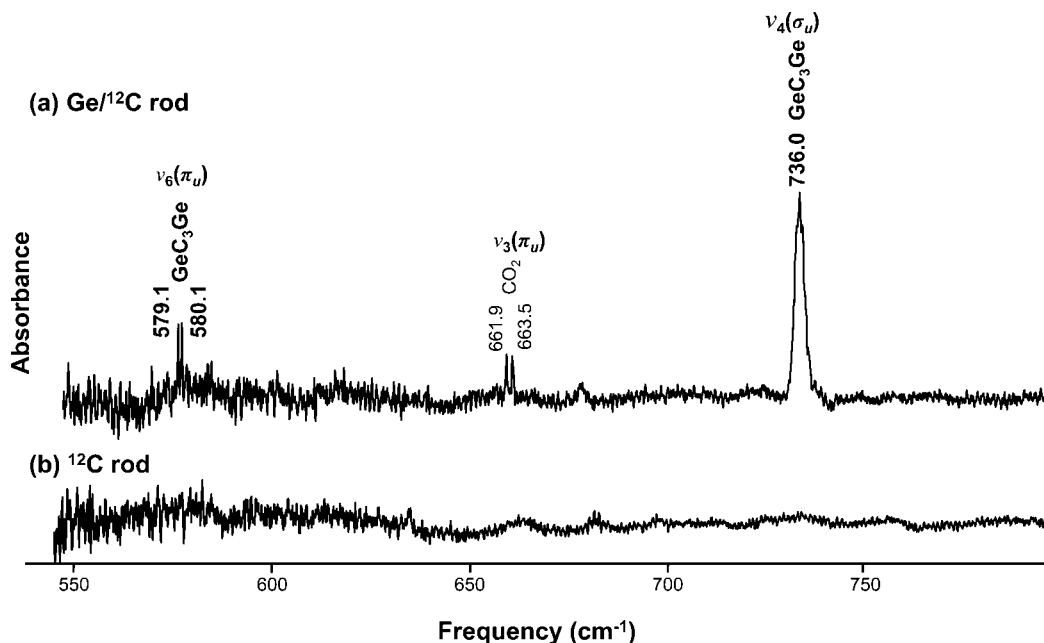


Figure 3. FTIR spectra produced by the ablation of (a) a germanium–carbon rod and (b) a pure ^{12}C rod in the 550–750 cm^{-1} frequency region.

TABLE 2: Observed Vibrational Frequencies (cm^{-1}) of the $\nu_4(\sigma_u)$ Mode for $^{70,72,73,74,76}\text{Ge}$ -Substituted Isotopomers of Linear GeC_3Ge , DFT Predictions at the B3LYP/cc-pVDZ Level of Theory, and Theoretical Predictions Given by Eq 2 Using the Optimized Mass Weighted Normal Mode Displacement Found by Minimizing the RMS Deviation of the Observed Frequencies

isotopomer		B3LYP/			
Ge-C-C-C-Ge	obsd	cc-pVDZ	scaled ^a	theoretical ^b	difference
76-12-12-12-76 (A)		738.1	733.4	733.9	
76-12-12-12-74 (B)	734.5	739.1	734.4	734.6	−0.1
76-12-12-12-73 (C)		739.6	734.9	735.0	
74-12-12-12-74 (D)	735.3 ^c	740.0	735.3	735.3	
76-12-12-12-72 (E)	735.3	740.1	735.4	735.3	0.0
74-12-12-12-73 (F)		740.5	735.8	735.7	
73-12-12-12-73 (G)		741.0	736.3	736.0	
74-12-12-12-72 (H)	736.0	741.0	736.3	736.0	0.0
76-12-12-12-70 (I)		741.2	736.5	736.1	
73-12-12-12-72 (J)		741.5	736.8	736.4	
72-12-12-12-72 (K)	736.7	742.0	737.3	736.7	0.0
74-12-12-12-70 (L)	736.7	742.1	737.4	736.8	0.1
73-12-12-12-70 (M)		742.6	737.9	737.1	
72-12-12-12-70 (N)	737.5	743.1	738.4	737.5	0.0
70-12-12-12-70 (O)	738.3	744.2	739.5	738.3	0.0

^a Results of the DFT-B3LYP/cc-pVDZ calculation scaled by a factor of $735.3/740.1 = 0.993514$. ^b Results of scaling by minimizing the rms deviation of the observed frequencies and the theoretical predictions given by eq 2. ^c Considered to be the unperturbed frequency in eq 2.

our assignment was still consistent with our assumption that the spectrum resulted from two equivalent germanium atoms we calculated the isotopic shifts using eq 2, minimizing the root-mean-square (rms) deviation between the calculated and observed frequencies. The optimized mass weighted normal mode displacement was found to be 0.2656, considerable lower than the DFT calculated value of 0.3124. The former value of the normal mode displacement was used to generate the semiempirical values for the germanium isotopic shifts shown in the “theoretical” column of Table 2 and the simulated spectrum exhibited in Figure 4b. The lower value of the normal mode displacement of the germanium atoms indicates, due to the normalization condition of the normal mode vector, that the

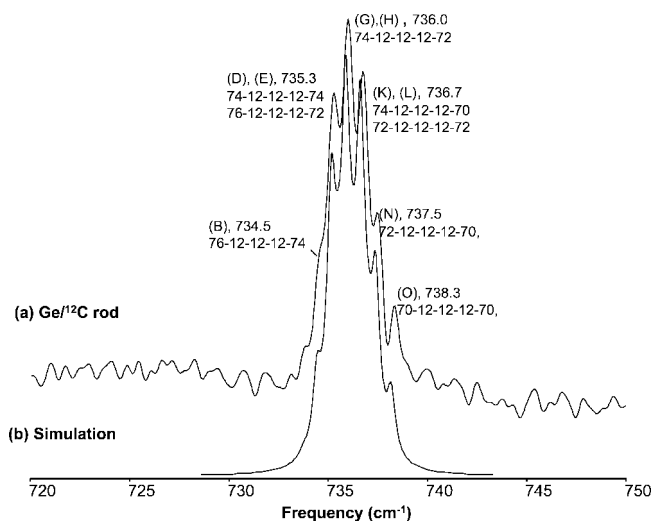


Figure 4. Comparison of the FTIR spectra of the $\nu_4(\sigma_u)$ mode of linear GeC_3Ge and its $^{70,72,73,74,76}\text{Ge}$ isotopic shifts (a) produced by the simultaneous evaporation of a germanium–carbon rod and with (b) a simulated spectrum calculated by using eq 2 and the calculated displacement vector of the Ge atoms obtained from minimizing the rms error between experimental frequencies and the ones obtained by using eq 2.

normal modes displacements of some or all the carbon atoms are larger than the DFT predictions. Thus it is expected that the observed ^{13}C absorptions should appear at lower frequencies than what is predicted by the DFT calculations. We will find below that indeed this is the case (e.g., see Figure 5).

In Figure 4b the spectrum is simulated by using Lorentzian profiles for the isotopomer shifts at the scaled frequencies given in Table 2. Each line profile is scaled by the predicted intensity of the isotopomer and its probability, given the natural abundances of the germanium isotopes. Table 2 compares the observed frequencies with the calculated scaled isotopomer frequencies and shows very good agreement between theory and experiment. The germanium isotopic shifts observed on the profile of the 736.0 cm^{-1} absorption band in Figure 4 prove that two germanium atoms participate in the vibration, but no

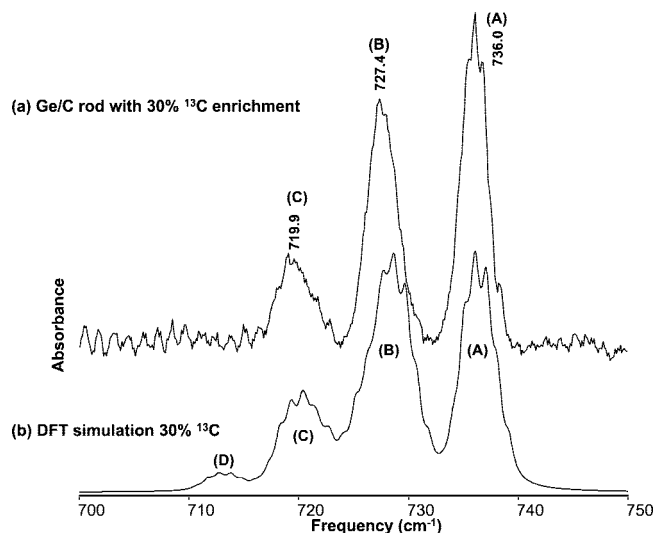


Figure 5. Comparison of the FTIR spectra of the $\nu_4(\sigma_u)$ mode of linear GeC_3Ge and its ^{13}C isotopic shifts (a) produced by the simultaneous evaporation of a germanium–carbon rod with 30% ^{13}C enrichment and with (b) a simulation for 30% ^{13}C and $^{70,72,73,74,76}\text{Ge}$ isotopomers derived from DFT calculations at the B3LYP/cc-pVDZ level. The letters correspond to the single and double ^{13}C -substituted isotopomers listed in Table 3.

TABLE 3: Comparison of Observed Vibrational Frequencies (cm^{-1}) of the $\nu_4(\sigma_u)$ Mode for ^{13}C -Substituted Isotopomers of Linear GeC_3Ge with the Predictions of B3LYP/cc-pVDZ Level Calculations

isotopomer Ge-C-C-C-Ge		obsd (cm^{-1})	B3LYP/ cc-pVDZ	scaled ^a	difference
Ge-12-12-12-Ge	(A)	736.0 ^b	741.0 ^b	736.0	
Ge-13-12-12-Ge	(B)	727.4 ^c	733.7 ^c	728.7	1.3
Ge-12-13-12-Ge					
Ge-13-13-12-Ge	(C)	719.9 ^d	725.4 ^e	720.5	0.6
Ge-12-13-12-Ge					
Ge-13-13-13-Ge	(D)		717.7 ^f	712.8	

^a Results of the DFT-B3LYP/cc-pVDZ calculation scaled by a factor of $736.0/741.0 = 0.9933$. ^b 74-12-12-12-72 isotopomer frequency. ^c 74-13-12-12-72, 74-12-12-13-72, 76-13-12-12-70, and 76-12-12-13-70 isotopomer frequencies (see text). ^d Center of the envelope. ^e 74-12-13-13-70 isotopomer frequency. ^f 74-13-13-13-72 isotopomer frequency.

conclusion can be drawn about the number of carbon atoms present. The presence of several unidentified germanium–carbon bands in the 1800–2200 cm^{-1} region, 2087.7, 2093.2, and 2116.6 cm^{-1} , raises the possibility that one of the species responsible for these bands might be responsible for the 736.0 cm^{-1} feature. Since DFT predicted intensities can sometimes deviate from experimentally observed intensities, the argument presented earlier linking the absorption at 736.0 cm^{-1} and the $\nu_3(\sigma_3) = 1920.7 \text{ cm}^{-1}$ fundamental of GeC_3Ge based on their intensity ratio is not conclusive. An experiment with a germanium–carbon rod enriched with ^{13}C was therefore carried out to establish the presence of three carbon atoms in a linear structure. The spectrum of Figure 5a obtained by the evaporation of a germanium–carbon rod with 30% ^{13}C enrichment shows two new absorptions labeled B and C.

Spectrum a in Figure 5 obtained on the evaporation of a germanium–carbon rod with 30% ^{13}C enrichment shows two new absorptions labeled B and C. Figure 5b shows the DFT simulated for linear GeC_3Ge spectrum for comparison. The absorption labeled A corresponding to Ge-12-12-12-Ge contains all the $^{70, 72, 73, 74, 76}\text{Ge}$ isotopomer absorptions as already

discussed and shown in Figure 4. The ^{13}C isotopic shifts are responsible for the absorptions labeled B (Ge-13-12-12-Ge and Ge-12-13-12-Ge), C (Ge-13-13-12-Ge and Ge-13-12-13), and D (Ge-13-13-13-Ge). The envelope corresponding to D was not observed since at 30% ^{13}C enrichment the abundance of the fully substituted isotopomer falls below the noise level. The DFT simulation predicts envelopes A, B, and C broader than those observed since the B3LYP/cc-pVDZ calculation predicts a higher value of the displacement vectors for the terminal germanium atoms. As can be seen in Figure 5 the observed carbon shifts are further away from the main band than the DFT calculations predict, indicating that some or all of the normal mode displacements of the carbon atoms are higher than the DFT predictions, as discussed above.

The envelope of the B absorption includes 27 isotopomers but only the feature at 727.4 cm^{-1} is clearly resolved. At the 0.2 cm^{-1} resolution the following isotopomers with their predicted abundances shown in parentheses could contribute to this feature: 74-13-12-12-72 (1.5%), 74-12-12-13-72 (1.5%), 76-13-12-12-70 (0.2%), 76-12-12-13-70 (0.2%), and 73-13-12-12-73 (0.09%). Since the absorption envelope labeled C and centered at 719.9 cm^{-1} is not resolved, no specific isotopomer assignments can be made in this case.

The results of isotopic shift calculations for linear GeC_3Ge structure are presented in Table 3, which together with Figure 5b shows the very good agreement between the observed and DFT calculated isotopomer frequencies. Comparison of measured ^{13}C and $^{70,72,73,74,76}\text{Ge}$ isotopic shifts with DFT predictions thus confirms that the absorption at 735.3 cm^{-1} (74-12-12-12-74) is the $\nu_4(\sigma_u)$ stretching mode of linear GeC_3Ge .

Table 1 indicates that the DFT calculations for linear GeC_3Ge predict the $\nu_6(\pi_u)$ bending mode at 575.4 cm^{-1} . Germanium atoms do not participate in this vibration, so a relatively sharp band is expected. As shown in Figure 3a the spectrum resulting from the evaporation of a Ge^{12}C rod has a pair of relatively narrow absorptions at 579.1 and 580.1 cm^{-1} that are obvious candidates for the $\nu_6(\pi_u)$ fundamental. The intensity ratio of this pair to the $\nu_4(\sigma_u) = 735.3 \text{ cm}^{-1}$ fundamental is 0.1, reasonably close to the 0.07 predicted. The 0.03 intensity ratio of the 580 cm^{-1} pair compared to the $\nu_3(\sigma_u) = 1920.7 \text{ cm}^{-1}$ fundamental is somewhat larger than the 0.007 predicted, but since the intensity ratio of 0.3 observed for $\nu_4(\sigma_u)$ to $\nu_3(\sigma_u)$ is also somewhat more than the 0.1 predicted, we suspect that the intensity predicted for the $\nu_3(\sigma_u)$ mode is a little high.

The 579.1, 580.1 cm^{-1} pair of absorptions with equal integrated intensity persist even after prolonged annealing at 20 and 40 K, leading us to discount two trapping sites as their origin and to consider the possibility that the degeneracy of the bending mode is broken. As can be seen in the spectrum in Figure 3a similar splitting is also observed for the $\nu_3(\pi_u)$ bending mode of CO_2 . In earlier work a similar pair of absorptions was observed, which at the time was different from the face centered cubic solid Ar although the two bands did not behave differently under annealing. Since this splitting, which is limited to bending modes, has now been observed for three different molecules, and the equal intensity of the peaks in each pair persists even after aggressive annealing, we are now inclined to think that the splitting results from the lifting of the degeneracy of the bending mode by the perturbation of the Ar matrix.

The splitting should also be observed in the ^{13}C isotopic shifts, and Figure 6 shows the spectrum when a germanium–carbon rod having 30% ^{13}C enrichment was used. The intensity ratios of isotopomer and main band are calculated by assuming that, consistent with the ^{13}C isotopic enrichment, the probability of

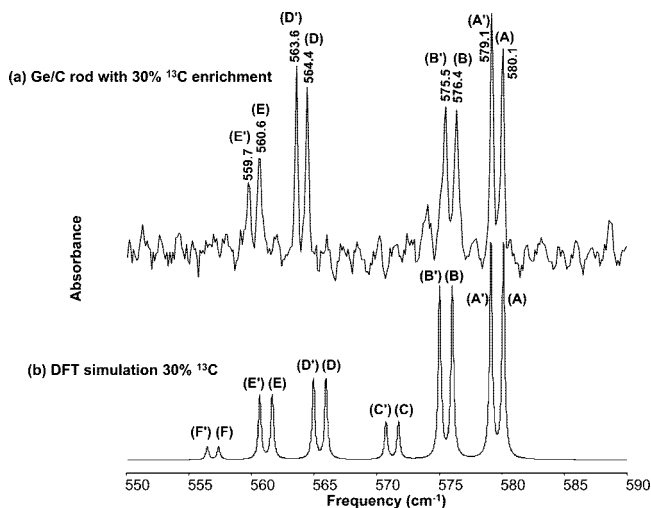


Figure 6. Comparison of the FTIR spectra of the $\nu_6(\pi_u)$ mode of linear GeC_3Ge and its ^{13}C isotopic shifts (a) produced by the simultaneous evaporation of a germanium–carbon rod with 30% ^{13}C enrichment and with (b) a DFT simulation for 30% ^{13}C enrichment derived from DFT calculations at the B3LYP/cc-pVDZ level. The letters correspond to the ^{13}C -substituted isotopomers listed in Table 4.

TABLE 4: Comparison of Observed Vibrational Frequencies (cm^{-1}) of the $\nu_5(\pi_u)$ Mode for ^{13}C -Substituted Isotopomers of Linear GeC_3Ge with the Predictions of B3LYP/cc-pVDZ Level Calculations

isotopomer Ge-C-C-C-Ge		obsd (cm^{-1})	B3LYP/ cc-pVDZ	scaled	difference
74-12-12-12-74	(A)	580.1	575.4	580.1 ^a	
	(A')	579.1	575.4	579.1 ^b	
74-13-12-12-74	(B)	576.4	571.3	576.0	−0.4
	(B')	575.5	571.3	575.0	−0.5
74-13-12-13-74	(C)		567.1	571.7	...
	(C')		567.1	570.7	
74-12-13-12-74	(D)	564.4	561.3	565.9	1.5
	(D')	563.6	561.3	564.9	1.3
74-13-13-12-74	(E)	560.6	557.0	561.6	0.9
	(E')	559.7	557.0	560.6	0.9
74-13-13-13-74	(F)		552.8	557.3	
	(F')		552.8	556.4	

^a Results of the DFT-B3LYP/cc-pVDZ calculation scaled by a factor of $580.1/575.4 = 0.99189$. ^b Results of the DFT-B3LYP/cc-pVDZ calculation scaled by a factor of $579.1/575.4 = 0.99361$.

evaporating a ^{12}C atom is 70% and that of a ^{13}C atom is 30%. As expected, the isotopic shifts appear in pairs that are approximately equidistant. The intensity of the pair labeled B, B' corresponding to the Ge-13-12-12-Ge isotopomer is $\sim 80\%$ of the main, Ge-12-12-12-Ge band labeled A, compared with the expected 86%. The intensity of the D, D' pair (Ge-12-13-12-Ge) is $\sim 62\%$ of the intensity of the main band compared to the expected 43%, and the E, E' pair (Ge-13-13-12-Ge) is $\sim 38\%$ compared to the expected 37%. The C, C' (Ge-13-12-13-Ge) and F, F' pairs (Ge-13-13-13-Ge), which should be respectively 18% and 8% as intense as the main band, fall below the noise level and cannot be observed. In general, the observed ratios are close to the expected values with a somewhat larger deviation for the D, D' pair that could be a consequence of incomplete randomization during the laser evaporation process or rod fabrication. This isotopic shift spectrum thus confirms the presence of three carbon atoms in a central symmetric structure.

The ^{13}C isotopic shifts calculated for the $\nu_6(\pi_u)$ bending mode of linear GeC_3Ge are shown in Table 4. Agreement between

theoretically predicted and experimentally measured isotopic shifts is very good. Figure 6 shows the DFT simulated spectrum calculated by simulating the spectrum for each of the frequencies for the A band and using the experimentally observed splitting. The experimentally observed spectrum matches the DFT simulated spectrum very well. This close agreement, together with the small difference between the theoretical and experimental intensity ratios for the three observed fundamentals, makes it possible to unambiguously assign the $\nu_6(\pi_u)$ bending mode of linear GeC_3Ge at 580.1 cm^{-1} . It is worth noting that the predicted $\nu_6 = 575.4 \text{ cm}^{-1}$ harmonic frequency is somewhat lower than the measured frequency; however, the relatively small effect ($\sim 2\text{--}10 \text{ cm}^{-1}$) is similar to what has been observed for other Group IV molecules previously studied including, for example, Si_3C_2 ,²³ Si_3C ,²⁴ Ge_5Ge ,²⁵ and C_{12} ,²⁶ and probably results from matrix effects and the DFT calculations.

6. Conclusion

Two new vibrational fundamentals of linear GeC_3Ge , $\nu_4(\sigma_u) = 735.3 \text{ cm}^{-1}$ and $\nu_6(\pi_u) = 580.1 \text{ cm}^{-1}$, have been assigned based on the results of ^{13}C and $^{70,72,73,74,76}\text{Ge}$ isotopic shift measurements and comparison with the predictions of DFT calculations at the B3LYP/cc-pVDZ level. This is apparently the first observation of germanium isotopic shifts in vibrational spectra.

Acknowledgment. Grants from The Welch Foundation (Grant P-0786), the TCU Research and Creative Activities Fund, and the W.M. Keck Foundation are gratefully acknowledged.

References and Notes

- (1) Robbins, D. L.; Rittby, C. M. L.; Graham, W. R. M. *J. Chem. Phys.* **2001**, *114*, 3570.
- (2) Kaolczak, J.; Harper, W. W.; Grev, R. S.; Clouthier, J. D. *J. Chem. Phys.* **1995**, *103*, 2840.
- (3) Leifeld, O.; Hartmann, R.; Miller, E.; Kaxiras, E.; Kern, K.; Grützmacher, D. *Nano* **1999**, *10*, 122.
- (4) Hartmann, R.; Gennser, U.; Sigg, H.; Ensslin, K.; Grützmacher, D. *Appl. Phys. Lett.* **1998**, *73*, 1257.
- (5) Todd, M.; Kouvetakis, J.; Smith, D. J. *Appl. Phys. Lett.* **1996**, *68*, 2407.
- (6) Ding, X. D.; Wang, S. L.; Rittby, C. M. L.; Graham, W. R. M. *J. Chem. Phys.* **1999**, *110*, 11214, and references cited therein.
- (7) Ding, X. D.; Wang, S. L.; Rittby, C. M. L.; Graham, W. R. M. *J. Phys. Chem. A* **2000**, *104*, 3712, and references cited therein.
- (8) Robbins, D. L.; Rittby, C. M. L.; Graham, W. R. M. *J. Chem. Phys.* **2004**, *120*, 4664.
- (9) Robbins, D. L.; Rittby, C. M. L.; Graham, W. R. M. *J. Chem. Phys.* **2002**, *117*, 3811.
- (10) (a) Presilla-Márquez, J. D.; Graham, W. R. M. *J. Chem. Phys.* **1994**, *100*, 181. (b) Rittby, C. M. L. *J. Chem. Phys.* **1994**, *100*, 175.
- (11) Presilla-Márquez, J. D.; Gay, S. C.; Rittby, C. M. L.; Graham, W. R. M. *J. Chem. Phys.* **1995**, *102*, 6354.
- (12) Presilla-Márquez, J. D.; Rittby, C. M. L.; Graham, W. R. M. *J. Chem. Phys.* **1996**, *104*, 2818.
- (13) Becke, A. D. *Phys. Rev. A* **1988**, *38*, 3098.
- (14) Perdew, J. P. *Phys. Rev. B* **1986**, *33*, 8822.
- (15) Lee, C.; Yang, W.; Parr, R. G. *Phys. Rev. B* **1988**, *37*, 785.
- (16) Frisch, M. J.; Trucks, G. W.; Schlegel, H. B.; Scuseria, G. E.; Robb, M. A.; Cheeseman, J. R.; Montgomery, J. A., Jr.; Vreven, T.; Kudin, K. N.; Burant, J. C.; Millam, J. M.; Iyengar, S. S.; Tomasi, J.; Barone, V.; Mennucci, B.; Cossi, M.; Scalmani, G.; Rega, N.; Petersson, G. A.; Nakatsuji, H.; Hada, M.; Ehara, M.; Toyota, K.; Fukuda, R.; Hasegawa, J.; Ishida, M.; Nakajima, T.; Honda, Y.; Kitao, O.; Nakai, H.; Klene, M.; Li, X.; Knox, J. E.; Hratchian, H. P.; Cross, J. B.; Bakken, V.; Adamo, C.; Jaramillo, J.; Gomperts, R.; Stratmann, R. E.; Yazyev, O.; Austin, A. J.; Cammi, R.; Pomelli, C.; Ochterski, J. W.; Ayala, P. Y.; Morokuma, K.; Voth, G. A.; Salvador, P.; Dannenberg, J. J.; Zakrzewski, V. G.; Dapprich, S.; Daniels, A. D.; Strain, O.; Farkas, M. C.; Malick, D. K.; Rabuck, A. D.; Raghavachari, K.; Foresman, J. B.; Ortiz, J. V.; Cui, Q.; Baboul, A. G.; Clifford, S.; Cioslowski, J.; Stefanov, B. B.; Liu, G.; Liashenko, A.; Piskorz, P.; Komaromi, I.; Martin, R. L.; Fox, D. J.; Keith, T.; Al-Laham, M. A.; Peng, C. Y.; Nanayakkara, A.; Challacombe, M.; Gill, P. M. W.; Johnson,

B.; Chen, W.; Wong, M. W.; Gonzalez, C.; Pople, J. A. *Gaussian 03*, Revision B.01; Gaussian, Inc.: Pittsburgh, PA, 2003.

(17) Martin, J. M. L.; El-Yazal, J.; Francois, J. P. *Chem. Phys. Lett.* **1995**, 242, 570.

(18) Rittby, C. M. L. (unpublished calculations for carbon chains—C_n, n = 3 to 21).

(19) Ding, X. D.; Wang, S. L.; Rittby, C. M. L.; Graham, W. R. M. *J. Chem. Phys.* **1999**, 112, 5113.

(20) Wielgus, P.; Roszak, S.; Majumdar, D.; Leszczynski, J. *J. Chem. Phys.* **2005**, 123, 234309.

(21) Shen, L. N.; Doyle, T. J.; Graham, W. R. M. *J. Phys. Chem.* **1990**, 93, 1597.

(22) Gonzalez, E.; Rittby, C. M. L.; Graham, W. R. M. *J. Phys. Chem.* **2006**, 125, 044504.

(23) Presilla-Márquez, J. D.; Rittby, C. M. L.; Graham, W. R. M. **6**, 104, 818.

(24) Presilla-Márquez, J. D.; Graham, W. R. M. *J. Chem. Phys.* **1992**, 96, 6509.

(25) Gonzalez, E.; Rittby, C. M. L.; Graham, W. R. M. *J. Chem. Phys.* **2006**, 125, 044504.

(26) Ding, X. D.; Wang, S. L.; Rittby, C. M. L.; Graham, W. R. M. *J. Chem. Phys.* **2000**, 112, 5113.

JP806370R